Nigerian Journal of Theoretical and Environmental Physics (NJTEP)
ISSN Print: 3026-9601
ISSN Online: 1597-9849
DOI: https://doi.org/10.62292/njtep.v4i3.2025.167
Volume 4(3), September 2026

Development of Petrophysical Modelling and 3D-Seismic Parameters in Volume Estimation of Reservoirs in Escravos-Warri Onshore Oil Field of Niger Delta in Nigeria

***[1]Ogundola Sunday, [1]Akinnubi Rufus Temidayo, [2]Temenu Funmilayo M. and [3]Tantasso Sabo**

[1]Adeyemi Federal University of Education, Ondo, Ondo state, Nigeria.
[2]Federal University of Technology, Akure, Ondo state, Nigeria.
[3]Federal Polytechnic, Mubi, Adamawa state, Nigeria.

[*]Corresponding author's email: ogundolsunday01@gmail.com

ABSTRACT
This study is aimed at identifying possible prospects and recoverable hydrocarbons within Temenu field, onshore Niger Delta using 3D seismic data and four viable well logs. These data were utilized for petrophysical analysis, structural interpretation, modeling and volumetric estimation of reservoirs delineation in the North-South direction of the field. Four reservoirs (Temenu A, B, C and D) were identified and their petrophysical properties were estimated. This research was carried out using the method of data sorting and loading, lithology identification, reservoir delineation, seismic-to-well tie, well-log correlation, fault mapping, horizon mapping, fluid distribution plot, reservoir modelling and volumetric computation. The results of the petrophysical analysis indicate a good porosity values which range from 19% to 39%. The permeability is very good ranging from 766mD to 9005mD, however, the water saturation ranges from 22% to 29%, while the hydrocarbon saturation varies from 71% to 78%. This shows that the reservoirs have enough pore spaces for hydrocarbon accumulation as well as effective interconnected migration pathway for fluid transmission within the pore spaces of the rocks. The modeled petrophysical parameters indicated that the reservoir rocks were hydrocarbon bearing. Estimation of the volume of the four reservoirs revealed good and productive zones. The most productive among the four reservoirs is reservoir C having a recoverable oil of 6, 855,786 MSTB.

Keywords:
Temenu Field,
Niger Delta,
3D Seismic Data
.

INTRODUCTION

Instability in the price of oil and gas often lead companies to focus on increasing their reserves through more precise definition and detailed characterization of reservoirs within the oil fields (Ojo *et al*., 2018). Reservoir characterization is a process for quantitatively assigning reservoir properties, such as porosity, permeability, and fluid saturations, while recognizing geologic information and uncertainties, in spatial variability (reservoir heterogeneity). Heterogeneity in a hydrocarbon reservoir is referred to as non-uniform and non-linear spatial distribution of rock properties such as porosity, permeability, and minerals saturation (Mohaghegh *et al*. 1996). The immediate application of reservoir characterization is useful in reservoir modelling and simulation and any primary and/or enhanced recovery design process in the petroleum and natural gas industry. Reservoir characterization methodologies have also been employed in environmental site remediation processes, where flows of contaminants in the earth's crust are being studied.

A reservoir's life cycle often begins with exploration that leads to discovery, which is followed by delineation of the reservoir, development of the field, and production by primary, secondary, and tertiary oil recovery methods.

Petrophysical parameters such as porosity and permeability are crucial in assessing different possible scenario within a reservoir. Seismic attributes are parameters that are computed, implied or derived from seismic data either by experiments, experience or logical reasoning. Some Seismic attributes quantify the morphological component of seismic data while others quantify the reflectivity component of seismic data. Morphological attributes are applied to extract information on reflector dip, azimuth, and terminations, which are related to faults, channels, fractures, diapers, and carbonate buildups. The reflectivity attributes extract information on reflector amplitude, waveform, and variation with illumination angle, which can be related to lithology, reservoir thickness, and the presence of hydrocarbons (Oyeyemi and Aizebeokhai 2015). While in the reconnaissance mode, 3D seismic attributes could be applied to rapidly delineate structural features and depositional environments. Whereas in reservoir characterization mode, 3D seismic attributes are calibrated against real and simulated well data to evaluate hydrocarbon accumulations and reservoir compartmentalization.

Taner *et al.*, 1979 have classified seismic attributes into geometrical and physical attributes. The geometrical attributes have the capacity to enhance the visibility of the geometrical characteristics of seismic events and are sensitive to lateral changes in dip, azimuth, continuity, similarity, curvature and energy. These are used in fault or structural interpretation and stratigraphic interpretation. However, the physical attributes enhance the physical parameters of the subsurface relating to lithology and stratigraphy for lithological classification and reservoir characterization. They include amplitude, phase, and frequency of seismic events. The magnitude of trace envelope is proportional to the acoustic impedance contrast; frequencies relate to bed thickness, wave scattering and absorption. Instantaneous and average velocities are directly related to rock properties. Delineation and development of subsurface hydrocarbon reservoir units, their interconnectivity, facies distribution, and reservoir properties constitute the basis of hydrocarbon exploitation, development and production.

Literature Review

The Niger Delta is situated on the Gulf of Guinea on the west coast of central Africa (Figure 2.1). The Delta is located in southern Nigeria, between Longitudes 3^0E – 9^0E, and latitudes 4^0 N – 6^0 N. It is bounded in the west by the Benin flank and in the east by the Calabar flank. It is bounded in the south by the Gulf of Guinea and in the north by Anambra Basin, Abakaliki uplift and Afikpo syncline in Figure 2.2 (Ejedawe, 1981). The delta extends in an east-west direction from southwest Cameroon to the Okitipupa Ridge. During the Tertiary it built out into the Atlantic Ocean at the mouth of the Niger-Benue river system, an area of catchment that encompasses more than a million square kilometres of predominantly savannah-covered lowlands. The delta is one of the world's largest, with the sub aerial portion covering about 75,000km^2 and extending more than 300km from apex to mouth (Doust and Omatsola, 1990). The regressive wedge of clastic sediments which it comprises is thought to reach a maximum of about 12km. throughout the geological history of the delta; its structure and stratigraphy have been controlled by interplay between rates of sediment supply and subsidence. Important influences on sedimentation rate have been astatic sea-level changes and climatic variations in the hinterland. Subsidence has been controlled largely by initial basement morphology and differential loading on unstable shale. The delta sequence is extensively affected by sedimentary and post sedimentary normal faults, the most important of which can be traced over considerable distances along strike. The resultant fault trends lie more or less parallel to the paleo geographic position of the delta front at each stage of its development, and are intimately related to the sedimentation pattern.

The evolution of the Niger delta is related to the development of the Ridge-Ridge-Ridge (RRR) triple junction and the subsequent separation of South American and African Continents (Short and Stauble, 1967). The area presently occupied by the Niger delta was the site of a RRR (ridge-ridge-ridge) triple junction during the Cretaceous (Figure. 2.3). The main sediment supply has been provided by an extensive drainage system, which in its lower reaches follow two failed rift arms, the Benue and Bida basins (Burke *et al*., 1971). Sediment input generally has been continuous since the late Cretaceous, but the regressive record has been interrupted by episodic transgressions. The bulk of the sediment was from the north and east during most of the Tertiary, even though there is little evidence for substantial Tertiary uplift in much of the catchment areas of the Niger-Benue river systems. According to Evamy *et al.*, 1978, the development of Tertiary Niger delta can be seen as a function of the rate of sedimentation (Rd) and rate of subsidence (Rs).

Evamy *et al.*, 1978 observed that variations in the relations of Rs and Rd result in the development of distinct sedimentary mega units of different shapes, extent and thickness.

Weber and Daukoru (1975) described the evolution of Niger delta in the following Phases: Pre-Santonian Basin Evolution, Santonian-Paleocene Basin Evolution, and Eocene –Recent Delta Phase. The oldest pre-Tertiary sedimentary basin, the Benue-Abakaliki Trough, originated as an arm of the triple-junction rift-ridge system that initiated the separation of South America from Africa in the Aptian/Albian (Burke *et al*, 1972). The three arms of the system opened up at different rates and different times. The opening started in the mid-Aptian by crustal stretching and down-warping accompanied by the development of coastal evaporated basins in the south Atlantic.

MATERIALS AND METHODS

This thesis aimed at the qualitative and quantitative interpretation of log data (Table 3.1), defines the lithology of prospective zones within the wells, locating reservoirs from non-reservoirs, delineating hydrocarbons, distinguish between oil and gas, evaluating the petrophysical parameters and correlation of the structural and stratigraphic units equivalent in time, age or stratigraphic position.

Materials Used for the Study

The materials used for this study include:

(i) Field base map: It is used to know the spatial location of the wells in the field, which subsequently aid the correlation of the wells.
(ii) Wireline logs: Four composite well logs comprising gamma-ray log, resistivity log, neutron and density log.
(iii) 3D-Seismic data
(iv) Check shot data

Method of Study

The various methods utilized in this study is presented in Figure 3.2. This shows the workflow of the study, starting with data sorting and loading, lithology identification, Reservoir delineation, seismic-to-well tie, well log correlation, fault mapping, horizon mapping, Fluid distribution plot, reservoir modeling and volumetric computation.

Well Log Analysis Procedures

Identification of Hydrocarbon Bearing Reservoirs

The hydrocarbon bearing reservoirs in the four wells were located, identified, named using the following procedure:

i) Boundaries of these reservoirs were established using gamma ray log.
ii) A relatively high resistivity value with the established reservoir defines a hydrocarbon-bearing reservoir.
iii) The reservoirs were then identified and the depth interval subjected to detailed study.

Determination of Gross and Net Productive Sand Reservoir Thickness

The gross reservoir thickness is determined by the interval covering both shale and sand with the reservoir shown by the gamma ray log, while, the net productive sand thickness is determined by subtracting the interval covering shale from the gross reservoir thickness.

Correlation

Correlation is defined as the determination of structural and stratigraphic units equivalent in age, time and stratigraphic position. The unit are delineated in vertical succession by distinct surfaces representing lithologic character. Well logs have the advantage of providing a continuous record over the entire well. Intervals of logs from different wells are matched for similarity or for characteristic log response to lithology markers, the marker units represented by sealing shales.

Most important, because stoned depth is recorded, there is no ambiguity as to the depth of the various markers. However, the log should respond to some property of the stratum that does not vary much from well to well. Well-to-well correlation studies thus permit accurate subsurface mapping and the determination of:

i) The elevations of formations present in the well relative to other wells.
ii) The thickening and thinning of lithologic sections; or lateral changes of sedimentation or lithology.
iii) Whether or not the well is within a given geologic structure.
iv) Whether well depth has reached a known productive horizon, and, if not, appropriate depth to be drilled.
v) The presence or absence of faults; dip, and fold.

The logs used frequently for correlation are the resistivity, SP, and gamma ray.

This thesis restricted its correlation analysis to the resistivity and gamma ray logs. The logs are vertically aligned with respect to a reference datum, (the mean sea level or any local equivalence), in other to establish the structural positions of the reservoirs.

Correlation Techniques

For initial quick look correlation, marker units represented by sealing shales are initially identified. Sand and carbonates are not laterally extensive owing to the way they are deposited. This is due to the fact that:

i. The clay and mud particles, which make up shale, are deposited in low energy environment which commonly cover large geographical areas. Therefore, shale curve signatures are often highly correlatable from well to well, and can be recognized over long distances.
ii. Prominent sand beds frequently exhibit significant variation in thickness and character from well to well, and are often laterally discontinuous.
iii. The resistivity signatures for the same sand on four well logs being correlated may be different as variations in fluid content in a sand bed may cause pronounced resistivity differences, (that is, water in contrast to gas).
iv. When the shale "base lines" have been determined, correlation of the sand deposits in between may be attempted. Where shales are not present in between sand layers, sand should be

correlated using the top of each sand formation, as the base may be erosive and therefore not a constant relative position.

Quantitative Interpretation

This involves the estimation of petro physical parameters such as porosity, water saturation, hydrocarbon saturation, permeability, movable hydrocarbon index, bulk volume water and residual oil saturation. Cross plots of the estimated parameters are generated to support the estimates.

Calculation of the gamma ray index is the first step to determining the volume of shale from a gamma ray log.

From Schlumberger (1974),

$$I_{GR} = \frac{GR_{log} - GR_{min}}{GR_{max} - GR_{min}} \quad (1)$$

Where: I_{GR} = gamma ray index

GR_{log} = Gamma ray reading of formation

GR_{max} = Maximum gamma ray (shale)

GR_{min} = Minimum gamma ray (clean)

And from Dresser, Atlas (1995) method, we have

$$V_{sh} = 0.083\{2^{3.71GR} - 1\} \quad (2)$$

For Tertiary Rocks (unconsolidated)

NOTE: This Dresser atlas method was used to suppress likely initial high response on gamma ray log to small amount of shale

The formation density compensated (FDC) and compensated neutron log (CNL) are two porosity, tools that were used to determined formation porosity.

Formation porosity was determined by substituting the bulk density reading on the FDC log into the equation below, for density:

$$\Phi_D = \frac{\rho_{ma} - \rho_b}{\rho_{ma} - \rho_f} \quad (3)$$

Where, $\rho_{ma} = 2.65 gm/cc$ (sandstone)

$\rho_{ma} = 1.09 gm/cc$ (Fresh water mud)

ρ_f = Formation bulk density

For Neutron, Φ_D is taken directly from the log. Therefore correction for shaliness is carried out using Hilchie (1981) equations.

$$\Phi_{N(COR)} = \Phi_N (V_{sh})(\Phi_{Nsh}) \quad (4)$$

$$\Phi_{D(COR)} = \Phi_D (V_{sh})(\Phi_{Dsh}) \quad (5)$$

Where Φ_N = Neutron porosity (from log)

Φ_D = Density derived porosity gotten form bulk density

V_{sh} = Volume of shale

Φ_{Nsh}, = Porosity of an adjacent shale

Formation effective porosity can be derived from Neutron and Density log using Schlumberger (1977)

$$\phi_{ND(COR)} = \sqrt{\frac{\phi^2_{N(COR)} + \phi^2_{D(COR)}}{2}} \quad (6)$$

From the Archie (1942) formula, estimation of formation factor is

$$F = \frac{a}{\phi^m} \quad (7)$$

For unconsolidated sand, as modified by Humble, we have

$$F = \frac{0.62}{\phi^{2.15}} \quad (8)$$

Where: F = Formation factor

ϕ = Porosity

m =Cementation factor

a =Tortuosity factor: a function of the complexity of the path the fluid must travel through the row. Using the Archie formula for water saturation; for clean, 100% water bearing sand formation.

$$S_w^n = \frac{FR_w}{R_t} \quad (9)$$

We have that,

$$S_w = 100\% = 1 \quad (10)$$

And,

$$R_t = R_O \quad (11)$$

Therefore,

$$R_w = \frac{R_O}{F} \quad (12)$$

$FR_w = R_O$ Is the resistivity of the 100% water filled sand formation. It is determined by sampling the clean water bearing reservoir at $10ft$ interval and averaging it, that is

$$R_{O=} \frac{\sum R_{ni}}{F} \quad (13)$$

Which represents the true resistivity of the zone.

For the estimation of water saturation in the uninvaded zone: The Archie formula for water saturation is

$$S_w = \sqrt{FR_w / R_t} \quad (14)$$

Therefore,

$$S_w = \sqrt{(R_0/R_t)} \quad (15)$$

Where: R_t = True resistivity of the formation

For the flushed zone,

$$S_{x0} = (S_w)^{1/5} \quad (16)$$

The moveable oil saturation was computed using the formula below:

$$MOS = S_{x_0} - S_w \quad (17)$$

This is the percentage of oil movable during invasion, which is expected to be high in a good reservoir with high porosity and permeability. The residual oil saturation was derived using the formula

$$ROS = S_H - MOS \quad (18)$$

This represents the percentage of oil left behind in the reservoir during invasion. For a reservoir with high porosity and permeability values, it is expected that most of the hydrocarbon would be moved by invasion, as such, its values should be low in comparison to that of movable oil saturation (MOS).

Estimation of resistivity index was computed using the formula

$I = R_t/R_0$ (19)

Where: $I = 1$; implies 100% water saturation.

Estimation of movable hydrocarbon index was derived using:

Where > 1 ; implies that hydrocarbon was not moved during invasion

$MHI < 0.7$(Sand stone: implies that hydrocarbon was moved during invasion

Estimation of bulk volume of oil was determined using the equation

$$BVO_{mov} = \Phi\left(S_{x_0} - S_w\right) = \Phi(MOS) \quad (20)$$

$$BVO_{unmov} = \Phi(1 - S_{x_0}) \quad (21)$$

Estimation of hydrocarbon pore volume is the fraction or percentage of the pore volume occupied by hydrocarbon; it was derived using the formula

$$HCPV = \Phi(1 - S_w) \quad (22)$$

$$= \Phi(S_H) \quad (23)$$

Estimation of irreducible water saturation was determined using Schlumberger equation (1989):

$$S_{wirr} = \sqrt{(F/2000)} \quad (24)$$

This described the small amount of water (formation or connate water), in percentage, that clings to the grains of the reservoir rock, as a result of capillary forces, that cannot be displaced by oil. At irreducible water saturation, water will not move, and the relative permeability to water equals zero; as a consequence, the reservoir will produce water free hydrocarbon (Morris and Biggs, 1967). Otherwise, increasing amounts of formation water (Swirr) takes up pore space, thereby, inhibiting the presence of other fluids and their ability to move through the rock.

The absolute rock permeability (in millin-darcy, md) at irreducible water saturation was determined using the empirical relationship proposed by Timur (1968).

$$K = \frac{0.136\Phi^{4.4}}{(S_{wirr})^2} \quad (25)$$

This represents the ability of a (reservoir) rock to transmit a single fluid when it is 100% Saturated with that fluid. From a more general empirical relationship proposed by Wyllie and Rose (1950), which incorporates irreducible water saturation and has the form

$$K = \frac{C\Phi^x}{(S_{wirr})^y} \quad (26)$$

Relative permeability (millidarcies) to oil was determined using the Park Jones (1945) relationships

$$K_{ro} = \frac{(1-S_w)^{2.1}}{(1-S_{wirr})^{2.1}} \quad (27)$$

Relative permeability to oil is the ration between the effective permeability of oil at partial saturation, and the permeability at 100% saturation (absolute permeability). With increasing relative permeability to oil, the reservoir formation will produce increasing amounts of oil (hydrocarbon) to water. Park Jones (1945) gave expressions for effective and relative permeability (md) to water as;

$$K_{rw} = \frac{(S_w - S_{wirr})^3}{(1-S_{wirr})^3} \quad (28)$$

It is measured as described above for oil but reference in this case is to water. When the relative permeability to water is zero, the formation will produce water free hydrocarbons. That is, the relative permeability to oil is 100%. Effective permeability to water as stated by Park Jones (1945) is

$$K_w = K_{rw}K \quad (29)$$

RESULTS AND DISCUSSION

Results are displayed in maps, logs, tables and graphs. The project reveals the Lithologies, identifies the reservoirs of interest and further study the productivity of the reservoirs. Petrophysical properties were estimated from the reservoirs mapped, the reservoir quality is determined. Lithologies identified from Temenu Field was done using gamma ray log, having scaled between the range 0 to 150 API and a cut-off of 75 API is set to differentiate the lithologies. Two different lithologies were delineated on the gamma ray logs, the shale lithology and the sand lithology. In order to correlate genetically related sand beds in this field, it is more effective to identify the sand beds from a single well and determine their properties as a reservoir. The Shale lithology is a region on the gamma ray log that exceeds the 75 API cut-off value, this displays as ash in colour and regarded has shale because of their high radioactive contents. The lithology is known to be porous but impermeable and they can serve as source rock for petroleum accumulation. Whereas Sand Lithology is a region on the gamma ray log that is below 70 API value, this displays as yellow in colour and are interpreted as sands because of their low radioactive contents. The lithology has the capacity of holding fluid and allows a free flow because it is porous and permeable.

Reservoirs were mapped by placing resistivity log with the gamma ray log in order to delineate the fluid content in the lithologies identified. Reservoir A, B, C and D was mapped across the well. The resistivity log accompanied with other logs such as the neutron and density log cross-plot is placed side by side with the gamma ray log in order to explain the fluid content of the reservoir. The fluid distribution across the wells was plotted to further explain the correlation**.**

In Temenu_04, Reservoir A has a depth range (6411 – 6470) ft, and a gross thickness of 51 ft (Figure 4.1). The lithology shows a log signature that is a cylindrical shaped sequence, having a sharp top and base. The deposit can be interpreted as a channel-fill reservoir sand. The reservoir is characterized with an average total porosity of 0.28 %, and the permeability of 3484mD which show a reasonable connectivity of the pore spaces for effective communication of the fluid within the pores. The reservoir is 15 % saturated with hydrocarbon, while the water saturation is 85% (Table 4.1). In Well 21, reservoir B falls within the depth of (5979 - 6100) ft. The gross thickness of the reservoir is about 121 ft, and the reservoir is identified to be aggraditional with Saw teeth form of sand deposits. Reservoir C is at an approximate top depth of 5692 ft and the base of the reservoir is at 5887 ft, the reservoir has a gross thickness of the reservoir is 195 ft thick (Fig.4.1).The gamma ray log signature of the reservoir is described as funnel shaped, coarsening upward sequence, having a gradational contact with the underlying shale. Thus, the reservoir is termed a bar finger sand deposit. The reservoir is identified as an excellent reservoir type because of its high porosity and permeability.

Table 1: Petrophysical evaluation of Temenu 04

Reservoir	GR(API)	Depth Intervals (MD) (ft)	Gross Thickness (ft)	Bulk Density (g/cc)	Total Porosity (%)	Effective Porosity (%)	Permeability (mD)	Water Saturation (%)	Hydrocarbon Saturation (%)
D	53.56	5570 – 5611	41	2.08	0.31	0.28	5762	0.22	0.78
C	72.11	5692-5887	195	2.12	0.30	0.24	3211	0.63	0.37
B	89.98	5979- 6100	121	2.10	0.31	0.19	3023	0.84	0.16
A	53.64	6411-6470	59	2.14	0.28	0.25	3484	0.85	0.15

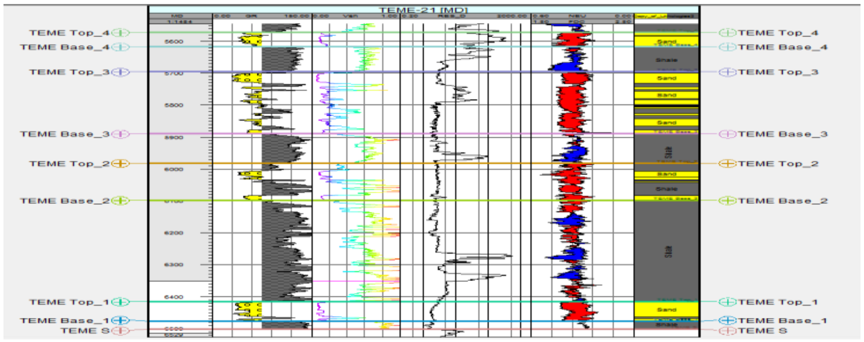

Figure 1: Reservoir Identification and Fluid discrimination in Temenu 04

Reservoir D falls within the depth interval 5570 ft – 5611 ft. It has an average thickness of 41 ft. The reservoir can be interpreted as delta front sheet sand deposit saturated with oil.

In Temenu_05, reservoir A falls in the depth (7077 – 7164) ft which has a gross thickness of 87 ft (Figure 4.2). The petrophysical evaluation revealed that the reservoir is has an average total porosity of 48 % and permeability value of 2256 mD (Table 4.2), but there is an omission in the data for the neutron and density log which makes it difficult to account for the hydrocarbon saturation of the reservoir. The reservoir is coarse up and has a sharp top which made it a funnel shaped deposit. The prograding nature of the sand deposit helped to infer a Crevasse splay.

Reservoir B is in the depth of (6493 – 6625) ft. The reservoir thickness is 132 ft (Figure 4.2). The log signature displays a serrated shaped pattern; having an aggradational contact with the underlying shale. The reservoir can be classified as a good reservoir because of its averagely high porosity and permeability of 25% and 1525 mD respectively (Table 4.2).

The top depth of the reservoir C is at an approximate depth of 6069 and the base depth at 6191ft, the reservoir has a thickness of 122 ft thick. On the gamma ray log signature, the reservoir sand serrated can be interpreted as a barrier beach deposit. In Temenu 05, reservoir D falls on a top depth of 5645 ft and the base is at 5695 ft.

The reservoir can be interpreted as a Channel filled deposit, having a total porosity of 29% and an average permeability of 3562 mD.

Table 2: Petrophysical Evaluation of Temenu 05

Reservoir	GR(API)	Depth Intervals (MD) (ft)	Gross Thickness (ft)	Bulk Density (g/cc)	Total Porosity (%)	Effective Porosity (%)	Permeability (mD)	Water Saturation (%)	Hydrocarbon Saturation (%)
D	47.87	5645-5695	50	2.12	0.29	0.26	3562	0.23	0.77
C	70.21	6069-6191	122	2.19	0.26	0.20	978	0.87	0.13
B	50.72	6493-6625	132	2.21	0.25	0.22	1525	0.88	0.12
A	44.41	7077-7164	87	2.23	0.48	0.41	2256	NIL	NIL

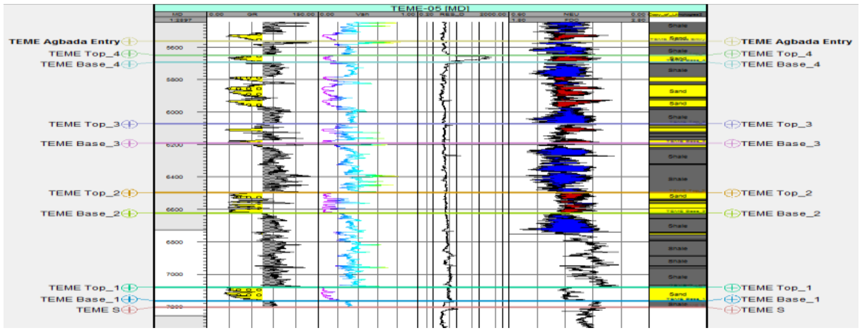

Figure 2: Reservoir Identification and Fluid discrimination in Temenu 05

In Temenu_06, Reservoir A is found within the depth interval (7277 – 7385) ft (Figure 4.3) with an average porosity value of 93% and the permeability of 9005 mD. The reservoir is 13% hydrocarbon saturated which can be classified as a low productive reservoir (Table 4.3). Rreservoir B in well-36 has a top depth of 6658 ft and the base depth is approximately at 6785 ft (Figure 4.3). The reservoir has a gross thickness of 127ft and an averagely high porosity and permeability of 80 and 8999 mD respectively. Hydrocarbons reserved in the reservoir is of low content probably because the reservoir might have been highly depleted as a result of exploitation or the fluid might have migrated to other reservoirs in the field due to suspicious leaking faults. Examining the log signature, the reservoir is identified as bell shaped, the sand lithology is a fining upward sequence having an abrupt contact with the underlying shale. Thus, the reservoir can be interpreted as a tidal inlet filled deposit.

Table 3: Petrophysical Evaluation of Temenu 06

Reservoir	GR(API)	Depth Intervals (MD) (ft)	Gross Thickness (ft)	Bulk Density (g/cc)	Total Porosity (%)	Effective Porosity (%)	Permeability (mD)	Water Saturation (%)	Hydrocarbon Saturation (%)
D	36.02	5787-5800	13	0.04	0.85	0.80	8912	0.62	0.38
C	80.66	6200-6344	144	0.05	0.79	0.78	8994	0.98	0.02
B	51.74	6658-6785	127	0.05	0.80	0.78	8999	0.99	0.01
A	50.58	7277-7385	108	0.02	0.93	0.91	9005	0.87	0.13

Reservoir C is at an approximate depth of 6200 ft and the base depth at 6344 ft, the reservoir has a thickness of 144 ft thick. The reservoir is classified a good reservoir type being fairly porous and permeable, saturated with hydrocarbon and mainly oil.
The well (Temenu 06) has its reservoir D at the top depth of 5787 2ft and the base depth is approximately at 5800 ft. The reservoir has a gross thickness of 13ft and an averagely high porosity and permeability of 85% and 8912 mD respectively. The reservoir is a tidal inlet fill deposit that has a fining upward sequence of an abrupt contact with the shale below it.

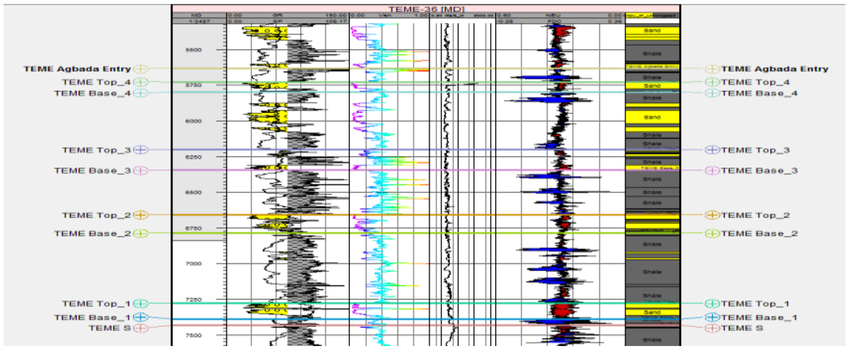

Figure 3: Reservoir Identification and Fluid discrimination in Temenu 06

In Temenu_07, Reservoir A is in the depth range of (7153 – 7270) ft (Figure 4.4). The reservoir has an average porosity value of 26% and the permeability 1472 mD that can be qualitatively described as very good but the hydrocarbon content has been depleted to 17% leaving the reservoir to be 83% saturated with water (Table 4.4). Reservoir B has a thickness of 141 ft, the top of the reservoir is at an approximate depth of 6560ft and has the base depth at 6701 ft. The reservoir is identified as a thick sand between shales, having an abrupt contact with the overlying and the underlying shales. The reservoir can be interpreted as a Crevasse splay deposits that have undergone a progradational process.

The top depth of the reservoir C is at an approximate depth of 6120 ft and the base depth at 6289 ft, the reservoir has a thickness of 169 ft thick. The top of channel deposit is said to be thin-bedded, indicating channel abandonment deposit. Reservoir D in Temenu 07 has a thickness of 62 ft, and its top depth is at 5685 ft, while the base is at 5747 ft. The Crevasse splay deposit is funnel shaped and it has an average total porosity of 82% and permeability of 3930 mD.

Table 4: Petrophysical Evaluation of Temenu 07

Reservoir	GR(API)	Depth Intervals (MD) (ft)	Gross Thickness (ft)	Bulk Density (g/cc)	Total Porosity (%)	Effective Porosity (%)	Permeability (mD)	Water Saturation (%)	Hydrocarbon Saturation (%)
D	51.04	5685-5747	62	2.14	0.28	0.24	3930	0.56	0.44
C	73.15	6120-6289	169	2.14	0.29	0.21	1416	0.61	0.39
B	49.94	6560-6701	141	2.16	0.27	0.23	2040	0.63	0.37
A	56.43	7153-7270	117	2.19	0.26	0.21	1472	0.83	0.17

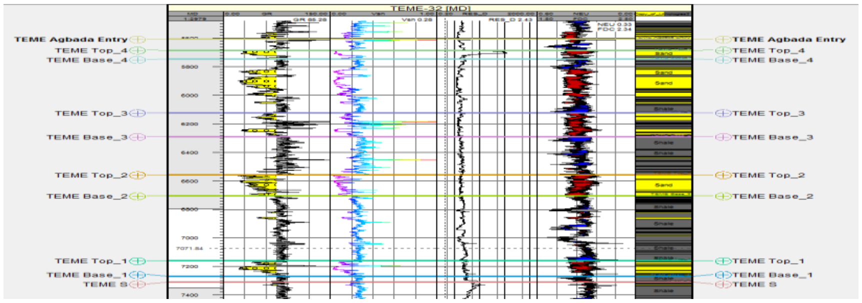

Figure 4: Reservoir Identification and Fluid discrimination in Temenu 07

In Temenu_08, reservoir A is in the depth range (7992-8089) ft (Figure 4.5), having an average porosity value of 26% and permeability of 766 mD (Table 4.5). The reservoir is coarsening upwards, giving it a funnel shaped deposit. It has a very good porosity and permeability values but the hydrocarbon content of the reservoir was not computed due to the absence of resistivity log in that depth interval.Reservoir B has its top at an approximate depth of 7296 ft and the base depth at 7430 ft, the reservoir thickness is 134 ft thick. The gamma ray signature describes the reservoir as blocky sand, having an abrupt contact with the overlying and underlying shales. Thus, the reservoir is interpreted as barrier beach deposit. The reservoir is classified as an excellent reservoir type being highly porous and permeable, saturated with hydrocarbon, mainly oil.

The reservoir is Oil reservoir sand, filled with oil down to shale. Reservoir C has a thickness of 159 ft and it starts from an approximate depth of 6822 ft and the base depth is at 6981 ft. The reservoir is interpreted as barrier beach deposit. The reservoir is classified as a good reservoir type being highly porous and permeable, which is fairly saturated with hydrocarbon. Reservoir D is found in Temenu 08 at an approximate top depth of 6333 ft and a base depth of 6400 ft, the reservoir has a thickness of 67 ft thick. The lithology is fining upwards and it can be identified as a barrier beach deposit. Petrophysical evaluation revealed a highly porous and permeable formation that is saturated with hydrocarbon.

Table 5: Petrophysical Evaluation of Temenu 08

Reservoir	GR(API)	Depth Intervals (MD) (ft)	Gross Thickness (ft)	Bulk Density (g/cc)	Total Porosity (%)	Effective Porosity (%)	Permeability (mD)	Water Saturation (%)	Hydrocarbon Saturation (%)
D	63.98	6333-6400	67	2.13	0.29	0.23	3016	0.88	0.12
C	83.03	6822-6981	159	2.14	0.28	0.18	1045	0.80	0.20
B	45.14	7296-7430	134	2.18	0.26	0.23	2215	0.58	0.42
A	57.80	7992-8089	97	2.18	0.26	0.21	766	NIL	NIL

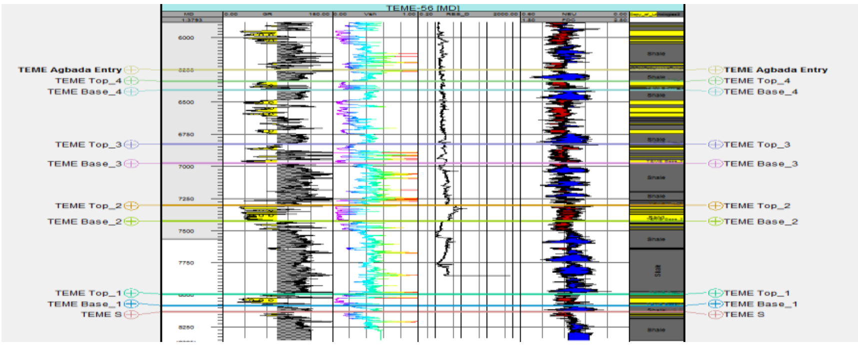

Figure 5: Reservoir Identification and Fluid discrimination in Temenu 08

Four reservoirs were mapped and correlated in Temenu-wells (04, 05, 06, 07, and 08) which trend in NW-SE direction (Figure 4.6). Well correlation was carried out relative to the shales that appear to be laterally continuous across the wells, while resistivity log was combined with gamma-ray log to delineate the reservoir beds. Reservoirs tops and bases were mapped across the wells on the basis of the relatively high resistivity values in the sand lithologies.

The well correlation has assisted in identifying individual reservoirs (sand bodies) that are present in the well by observing intervals where the gamma ray log reads relatively low values (i.e. deflection to the left). The reservoirs varied in thicknesses, some were hydrocarbon bearing while some were water bearing as displayed in the reservoir fluid plots in Figures (4.7 – 4.10).

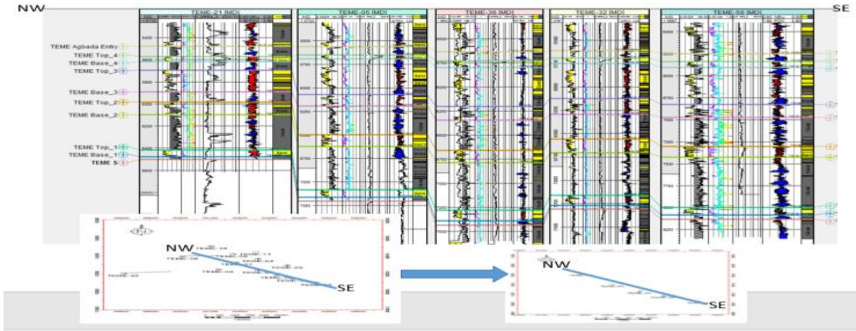

Figure 6: Well Log Correlation Panel for well (Temenu 04, 05, 06, 07 and 08).

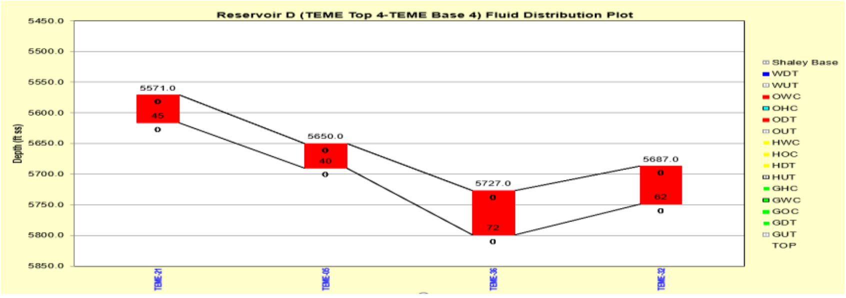

Figure 7: Reservoir D Fluid Plot showing the distribution of Fluid within Well 04, 05, 06, 07 and 08

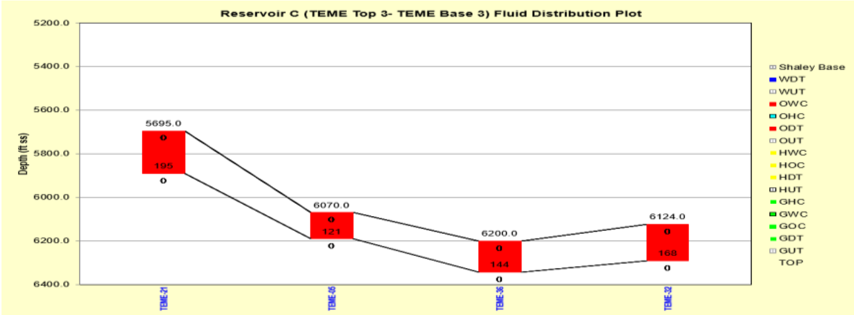

Figure 8: Reservoir C Fluid Plot showing the distribution of Fluid within Well 04, 05, 06, 07 and 08

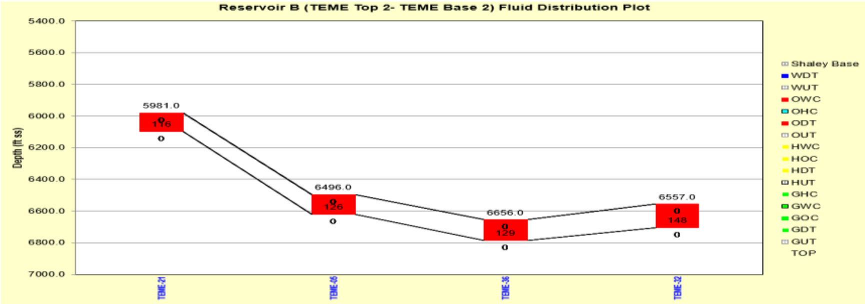

Figure 9: Reservoir B Fluid Plot showing the distribution of Fluid within Well 04, 05, 06, 07 and 08

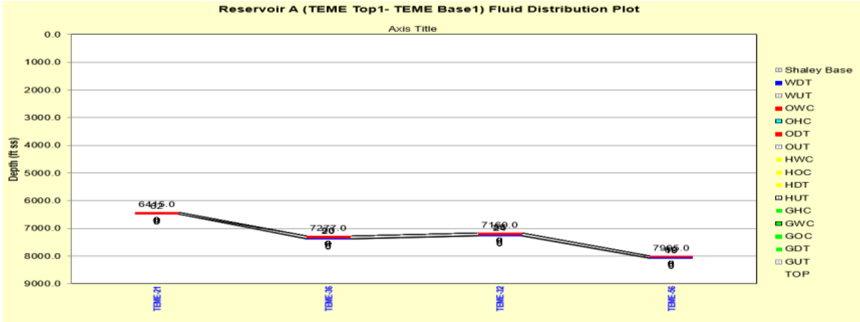

Figure 10: Reservoir A Fluid Plot showing the distribution of Fluid within Well 04, 05, 06, 07 and 08

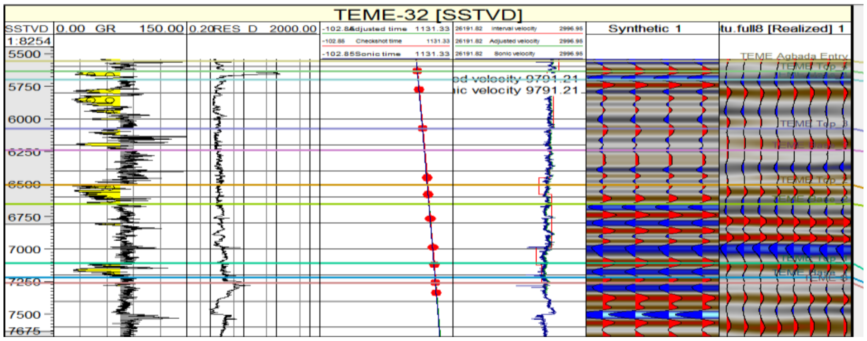

Figure 11: Synthetic Seismogram for Well 07 (Well 32)

Geological structures (Faults and Horizons) were mapped from the integrated 3D seismic data and well logs. The faults are geologic structures that could serve as barriers to the flow of hydrocarbons or pathways for fluid flow. The visible reflection lines that represent the tops and bases of reservoirs identified on wells are mapped out on the seismic sections as time surfaces, and converted to depth map using lookup function (a relationship between time and depth) generated from the checkshots data.

Several fault lines were picked from the seismic inline sections at every 5 steps interval (Figure 4.12). Four major faults (F1, F2, F3 and F4) were identified and displayed on the seismic sections (Figure 4.13). The faults trend from Northeast- Southwest on the inline sections.

Subsurface structural maps show relief on a subsurface horizon with contour lines that represent equal time/depth below a reference datum or two-way time from the surface. These contour maps reveal the slope of the formation, structural relief of the formation, its dip, and also faulting or folding patterns.

The time surface map named Temenu 04 lies within the time range of 1350 ms to 1825 ms and its base has contour values that range 1400ms to 1950ms. There structural highs were observed at the northern central portion of the field. The major faults ‘F1 and F2’ cut across the peak of an anticlinal structure, whose time values decreases inward forming a closure on the fault. The depth converted versions of the Temenu A top and base have their contour values range 4800 ms to 6800 ms and 5000 ms to 6900ms.

Horizon ‘B’ top time map lies within the time range of 1450 ms to 1950 ms contour values, while the base is 1500ms to 1975ms.

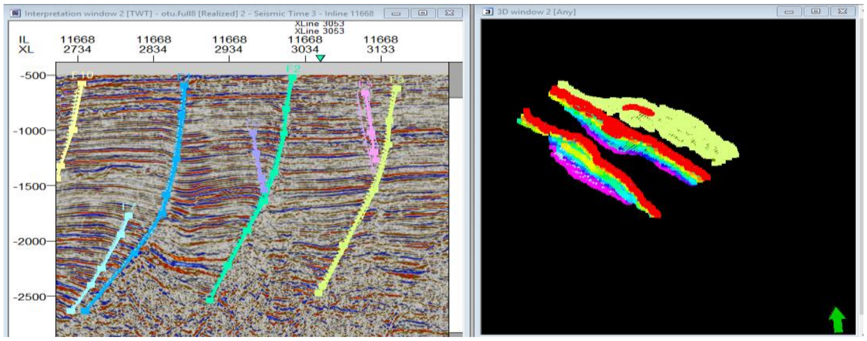

Figure 12: Fault mapping on Inline 11668 seismic section

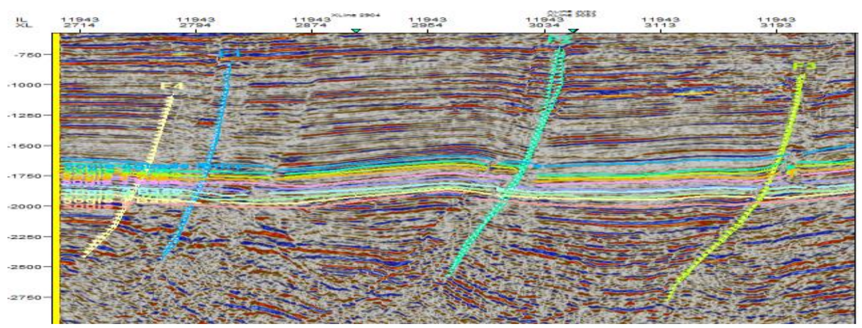

Figure 13: Extensive Faults Mapped in the Field

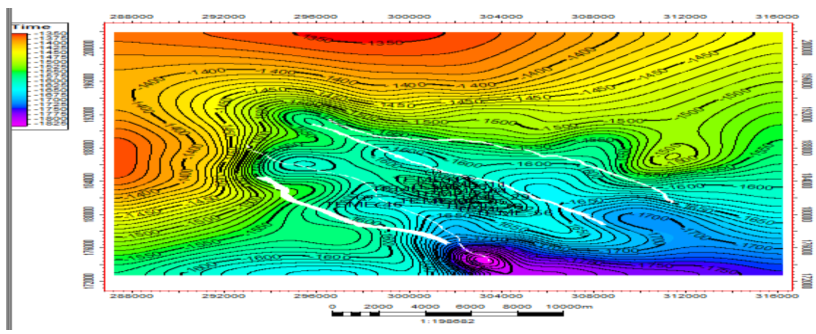

Figure 14: Surface Time Map of Temenu A Top

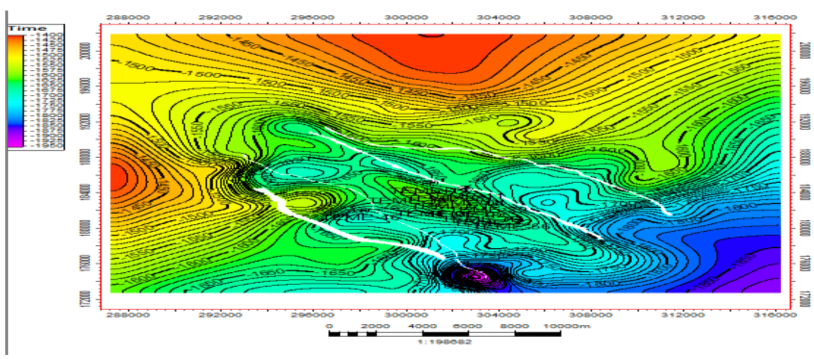

Figure 15: Surface Time Map of Temenu A Base

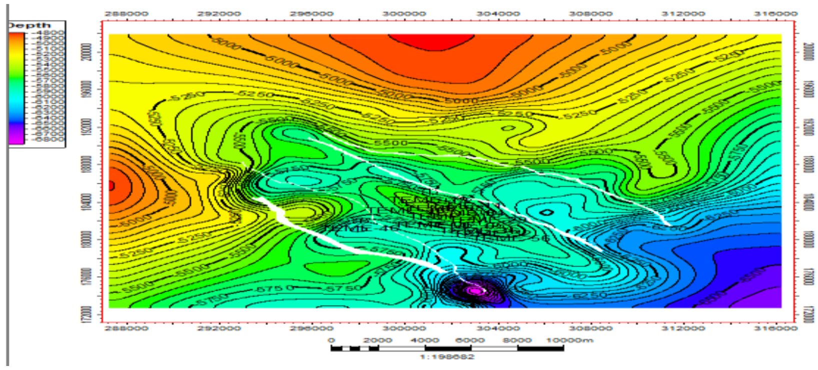

Figure 4.16: Temenu A Depth Map Top

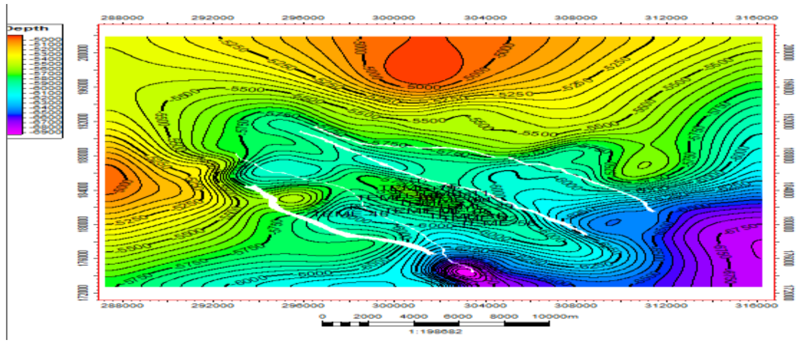

Figure 17: Surface a Base Depth

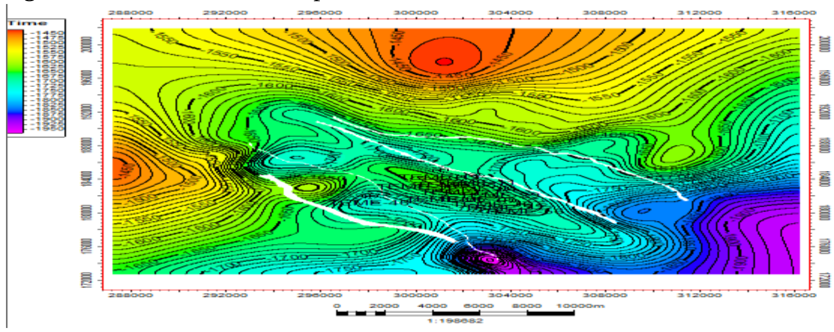

Figure 18: Time Surface Map B Top

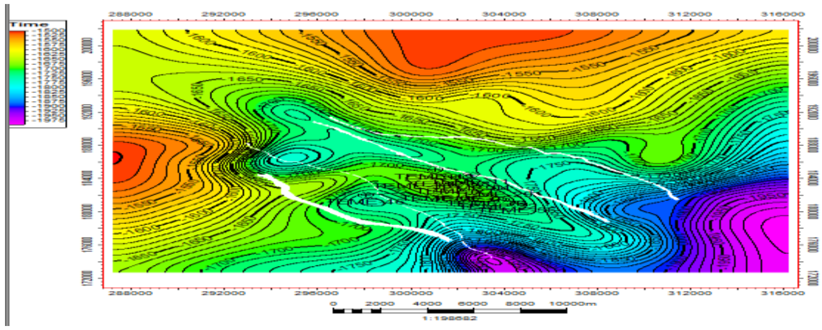

Figure 19: Time Surface Map of B Base

The structural high is observed at the northern central portion of the field. Fault 'F1 and F2 which are continuous faults in the field cut across the peak of an anticlinal structure, whose time values decreases inward forming a closure on the fault. The converted depth map has the top contour range of 5200ms to 7000ms, while the base has its range from 5300ms to 7200ms.

Horizon 'C' top time map is within the contour range of 1525 ms and 2050ms, while the base has contour 1600ms to 2150ms. The major fault F1 and F2 pass through the peak of the structural high that forms an anticline in the field. Converting horizon C to depth, the top of the reservoir has contour range 5450ms to 7350ms, and the base contour range is 5500ms to 7400ms.

Horizon 'D' top time map is within the contour range 1575 ms to 2075 ms, while the base has contour range of 1575ms to 2100ms. The mapped surfaces reflect a structural high towards the northern and central portion of the maps. The faults F1 and F2 cut through the two surfaces at the anticlines. The top of the converted time surface to depth has its top range 5600ms to 7600ms and the base is contoured within the range 5950ms to 7800m A geologic 3D grid generation is the first step to build and is a network of horizontal and vertical lines used to describe a three dimensional geological model.

Pillar gridding is the process of generating the grid, which represents the base of all modeling. The skeleton is a grid consisting of top, mid and base skeleton grids (Figure 4.30). It specifies the variation of the petrophysical properties. The result from pillar gridding is the main skeleton designated as top, mid and base skeletons.

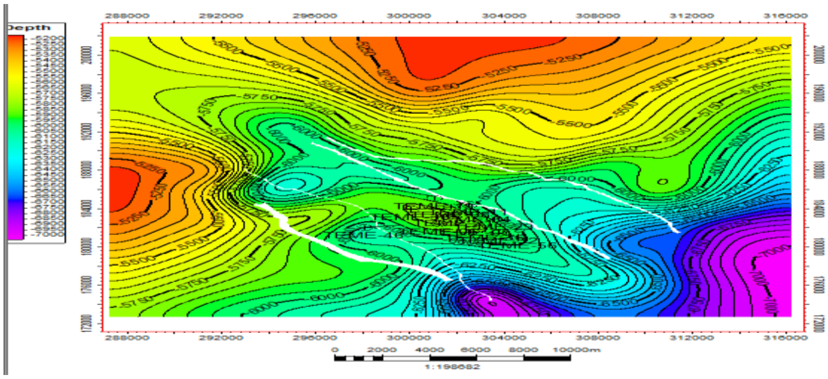

Figure 20: Depth Map of Top B Surface

CONCLUSION

The search for hydrocarbon is becoming increasingly more difficult and expensive and there is an insatiable thirst for oil and gas consumption worldwide. An increase in production is essential and part of the ways this can be made possible through effective reservoir characterization and modelling. The data used include 3D seismic and well logs from four wells. These data Information were utilized for the petrophysical analysis, structural interpretation, modeling and volumetric estimation of reservoirs delineated and correlated across the North- South direction of the field. On this field, four reservoirs (Temenu A, B,C,and D) were identified and their petrophysical properties were estimated. The results of the petrophysical analysis indicate a good porosity values which range from 19% to 39%. The permeability is very good ranging from 766mD to 9005mD, however, the water saturation ranges from 22% to 29%, while the hydrocarbon saturation varies from 71% to 78%. This shows that the reservoirs have enough pore spaces for hydrocarbon accumulation as well as effective interconnected migration pathway for fluid transmission within the pore spaces of the rocks. Finally, the application of well logs and 3D seismic data for this study over Temenu field has shown their effectiveness in detecting the presence of hydrocarbon and delineating geologic structures.

Recommendation

It is important to carry out fault sealing assessment of this field in order to unravel the connectivity of the reservoirs. Further interpretation such as seismic attribute analysis, AVO analysis, seismic inversion, rock physics, etc. should be carried out on the field so as to affirm the existence of hydrocarbon and the tapping mechanism in this field. Uncertain analysis such as Monte Carlo stimulation, material balance analysis, etc. should also be used to further evaluate and affirm the STOIIP value. This will help to affirm if the field is economically fit for exploitation. More wells should be drilled along the west and east direction of the field. This will help in the proper optimization of the field.

Acknowledgement

We are grateful to the management of Adeyemi Federal University of Education, (AFUED), Ondo , Ondo state for giving us express approval to benefit financial supports from Tertiary Education Trust Fund (Tetfund) in order to carry out this institution-based research.

REFERENCES

Abe, S. J., Ayuk, M. A., Ojo, B. T., Oluwadare, O. A., and Olowokere, M. T., (2016), A Study of Seismic Hydrocarbon Indicators over X field, Niger Delta. Journal of Bassic and Applied Research International (JOBARI) 16(3): pp 202-210. (United Kingdom, 20% Contribution). https://doi.org/10.19820/1.17853

Adewumi R.O (2013) Exploration Rock Physics: The link between geological processes and geophysical observables. J. Applied Geophysics Vol.23 pp.56-89. https://doi.org/19.2860/1.18943

Ako B. D., Amigun J., and Adelusi A. O., (2004). The Application of Integrated Geophysical Methods in oil Sand Exploration in Agbabu Area of Southwestern Nigeria. Corpus ID: 134508400. https://doi.org/11.8970/1.178421.

Anstey K. G (1973) Statistical Rock Physics for seismic Reservoir characterization. Pp 34-67. https://doi.org/12.1982/1.178532

Archies, G. E., (1942). The Electrical Resistivity Log as an Aid in Determining some Reservoir Characteristics. *Petroleum Technology*. Pg. 5, 54-62 https://doi.org/10.17854/1.1456424.

Bilotti, F. D., J. H. Shaw, R. M. Cupich, and R. M. Lakings, (2005). *Detachment fold, Niger Delta,* in J. H. Shaw, C. Connors, and J. Suppe, eds., Seismic interpretation of contractional fault related folds: AAPG Studies in Geology 53, p. 103– 104. https://doi.org/13.18720/1.1784321

Bouvier, J. D., Kaars-Sijpesteijn, C. H., Kluesner, D. F., Onyejekwe, C. C. & Van der Pal, R. C. (1989). *Three-Dimensional Seismic Interpretation and Fault Sealing Investigations, Nun River Field, Nigeria.* https://doi.org/11.92170/1.76321

Coffeen M.U (1984). Seismic interpretation of Tomboy Field, Offshore Western Niger Delta. International Journal of science and Technology (IJST), 2(9): 649.

Daniel M.H (2003) .The log Analyst and the programmable pocket calculator .The Log Analyst Vol. 18, pp. 3-11. https://doi.org/5.4510/1.187021

Daukoru, E. and Weber, K. J. (1975). Petroleum Geology of Niger Delta. Journal of Mineral Geology, Vol 12, 9-12. https://doi.org/12.1230/1.74321

Dobrin M.J (1988). Gravity field and structure of the Niger Delta , Nigeria , West Africa . Geological society of America Bulletin Vol. 76 pp407-422 Kaplan 1994. https://doi.org/19.1860/1.90431

Doust H. and Omatsola E., (1990). *Niger-Delta, in J.D Edwards, and P.A Santogrossi, eds.Divergent /passive margins basins:* AAPG Memoir 48, pp. 201-238. https://doi.org/7.18700/1.893127.

Ekweozor and Okoye (1980) Petroleum source bed evaluation of Tertiary Niger Delta. Department of Energy Canada. https://doi.org/17.1542/1.178540.

Emery K. and Benkhelil, J., (1975). The Origin and Evolution of the Cretaceous Benue Trough. Elsevier Scientific Publishing. Pp 2214, https://doi.org/14.16732/1.89410

Frankland E. J., and Cordry E. A., (1967). The Niger Delta Oil Province. Recent Development Onshore and Offshore. Practical Seventh World Petrol Cong. 195-209.. https://doi.org/16.1871/1.168321

Gallango, O., (2002). The Petroleum System of the Central Perija Fold Belt, Western Venezuela. AAPG Bulletin 86(7). https://doi.org/10.136/61EEDC74-173E-11D7-8645000102C1865D

Haack R.C, Sundararaman P., Dahl J. (2002). Niger Delta Petroleum system: Presented at the 2003 AAPG/ABGPHedberg Research symposium, Reo dejaneiro, Brazil, ext. Abstract. https://doi.org/15.1984/1.178643

Halliburton Energy Services (2001). Log interpretation Charts, Houston, Texas Halliburton Company.

Hilchie D.W (1978) Applied Openhole Log Interpretation: Golden Colorado, D.W, Hichie Incorporated pp 309. https://doi.org/14.1870/1.187650

Magoon, B. L., and Edward A. B., (2003). Petroleum Systems. http://bookstore.aapg.org

Matava, T., and Rooney, M., (2003). Migration effects on the composition of hydrocarbon accumulations in the OML 67-70 areas of the Niger Delta. https://doi.org/10.1306/02190300116

MicheleL. W., and Tuttle R. R., Charpentier, and Micheal E. (1999). Niger Delta Province, Nigeria, Cameroon and Equatorial Guinea Africa. https://doi.org/10.1780/1.1476214.

Nwachukwu, J. I., and Odjegba (2001). Geology of Niger Delta Basin. https://doi.org/10.1016/B978-0-12-812161-0.00002-8. https://doi.org/8.7890/1.1572106

Olisa, B. A., Ojo B. T., and O. A Oluwadare, (2018): 2-Dimensional Seismic Interpretation of 'X-Field" in the Niger Delta. Journal of Geology and Geophysics- JAGG (International Organization of Scientific Research-IOSR. https://doi.org/11.1641/1.187414.

Ojo, B. T., Olowokere, M. T., and Oladapo, M. I., (2018). Quantitative Modeling of the Architecture and connectivity properties of reservoir in Royal Field, Niger Delta. Journal of Applied Geology and Geophysics JAGG (International Organization of Scientific Research-IOSR Journal DOI: 10.9790/09900602020110. https://doi.org/13.6597/1.1310714.

Omatsola, M. E., (1982). Petroleum geology of Niger Delta. Shell International Petroleum Nigeria. The Hague, Netherlands. Journal of Geosciences and Geomatics. https://doi.org/7.43120/1.1563109.

Ozumba CI, Ozumba MB, Obobaifo CE (1999). *Striking a balance between Oil Exploration and Protecting the Environment.* NAPE Bull 14(2):130–135. https://doi.org/3.67021/5.639871.

Petrol consultants, (1996). Petroleum Exploration and Production Database: Petrol consultants, Inc., P.O. Box 740619, Houston TX. https://doi.org/17./1.5643201

Schlumberger (1989). *Log Interpretational Principle/Applications; Schlumberger EducationalServices,* order no. SMP-7017, Houston. Schlumberger well services 1989. Log Interpretation, Principles /Application, 209-221. https://doi.org/1.1190/1.1465491.

Schmidt, I., M. Docherty, F. Pauget, and Lacaze. S. (2010*). Improved 3D Seismic Interpretation and Reservoir Model Construction using PaleoScan Technology*. *SEG*, Vol.3, 200-250. https://doi.org/16.1190/1.129853.

Short, K. C. and Stauble, A. J. (1967). *Outline of geology of Niger Delta. American Association of Petroleum Geologist Bulletin,* v.51, pp. 761-799. https://doi.org/12.3241/1.167210

Stoneley, R., (1966). The Niger Delta Region in the light of the Theory of Continental Drift. Cambridge University Press.

Taner M. T. Neboh Tselludi, Bortch Shelfieds (1979) Complex Seismic Trace Analysis. Society of Exploration Geophysics. https://doi.org/10.1190/1.1440994.

Telfold, W. M., Gelbart, L. P., and Sheriff, R. E., (1990). *Applied Geophysics*. First Edition Cambridge: pp 442-457; 468-472. https://doi.org/16.1697/1.1860231.

Timur A.T (1968). *Striking a balance between Oil Exploration and Protecting the Environment.* NAPE Bull 14(2):130–135. https://doi.org/15.2319/4.1856320

Whiteman, G., (1998). Geology, geochemistry and origin of the banded and granite gneisses in the basement complex of the Ilesha area, southwestern Nigeria. Journal of African Earth Sciences. Pp 633-641. https://doi.org/17.7521/1.1487201

Wyllie M.R and Rose A.Y (1950) An experimental investigation of factors affecting elastic wave velocity in porous media Geophysics , 28 pp 459-493. https://doi.org/15.1143/1.13298794.